Вісник Тернопільського національного технічного університету
https://doi.org/10.33108/visnyk_tntu
Scientific Journal of the Ternopil National Technical University
2025, № 2 (118) https://doi.org/10.33108/visnyk_tntu2025.02
ISSN 2522-4433. Web: ***visnyk.tntu.edu.ua***

UDC 621

PROBLEMS OF INTAKE AIR FILTRATION FOR COMBUSTION ENGINES OF VEHICLES

Tadeusz Dziubak[1]; Jan Dizo[2]

[1]Military University of Technology, Warsaw, Poland
[2]University of Zilina, Žilina, Slovakia

Abstract. *Abstract: The basic method of protecting the engine against the destructive effects of mineral dust sucked in with the air intake to the engine are air filters. Passenger cars will be equipped with single-stage filters with a filter insert (porous partition) in the form of a panel made of pleated filter paper. Filter papers show insufficient filtration accuracy of dust grains below 5 μm. The principles of shaping traditional filter partitions made of pleated filter paper and the principles of selecting a filter insert for a car engine using the criterion of permissible filtration speed are presented. The principle of operation and construction as well as the properties of filters with axial air flow, which are made in the modern PowerCore technology, are shown, which reduces the filter dimensions, at the same time resulting in lower pressure drop and greater dust absorption, and therefore a longer period of operation. The article pays special attention to the properties of nanofibers, which are produced from polymers using the «electrospinning» technology, and their filtration properties enable the improvement of the efficiency and accuracy of engine intake air filtration. The results of experimental tests of the efficiency and accuracy of filtration and pressure drop performed for several filter beds differing in structure parameters are presented. It has been shown that the nanofiber layer significantly increases the efficiency and accuracy of filtration of dust grains below 5 μm. Low filtration parameters of the filter beds in the initial filtration period have been demonstrated, which negatively affects engine wear.*

Key words: *air pollution, combustion engines, air filter, separation efficiency, dust absorption, filtration accuracy, pressure drop.*

https://doi.org/10.33108/visnyk_tntu2025.02.020 *Received 09.01.2025*

1. INTRODUCTION

Internal combustion engines, which are the driving units of motor vehicles, suck in significant amounts of atmospheric air during operation under rated conditions in order to ensure proper fuel combustion and achieve the required performance. The intake systems of passenger car engines suck in 150–400 m^3 of air per hour. The air flow for truck engines has a value in the range of 900–2000 m^3/h. Special vehicle engines (tanks, transporters), due to their large displacement, suck in 3000–6000 m^3/h. Along with the intake air, a considerable mass of various solid pollutants enters the cylinders of internal combustion engines of motor vehicles, the main component of which is mineral dust (road dust), which is lifted from the ground to a considerable height by moving vehicles. Dust from the ground can be carried to considerable heights by the wind. The two main components of road dust determine its chemical properties, they are silica SiO_2 and alumina Al_2O_3. Their total share of dust reaches 95%. The residues are: Fe_2O_3, MgO, CaO. K_2O, Na_2O and moisture [1–3]. The chemical composition is close relation to the composition and type of substrate, as well as the location and altitude above the ground. The chemical composition of dust depends on climatic factors, as well as dust that has entered the atmosphere as a result of forest fires, landfills, industrial activities and volcanoes, and then falls by gravity.

 Corresponding author: Tadeusz Dziubak; e-mail: tadeusz.dziubak@wat.edu.pl

Road dust, like other dust found in nature, has the characteristics of polydisperse dust. This means that dust grains of different sizes are found in the dust, and their relative share in the total mass of dust is determined by the granulometric composition (fractional composition), which, like the chemical composition, depends on the type of substrate and the height above the ground. This is due to the residence time of mineral dust grains in the air, which depends on the speed of their descent. Due to their varying diameters and different densities, dirt particles have different masses and therefore fall to the ground at different speeds. During gravitational descent, the particles are affected by the drag force of the air, which is directed in the opposite direction and inhibits the descent. Therefore, the interrelation between the gravitational force and the drag force of the medium is important. The speed of descent increases significantly as the grain diameter and material density of the particle increases. Particles smaller than 0.1 μm are subject to random Brownian motion due to collisions with gas particles and with other dust particles, whose motion in turn is mainly caused by moving gas particles. Particles with conventional sizes of 0.1 to 1 μm show low falling velocities in still air, while particles larger than 1 μm show small but noticeable falling velocities. The falling velocities of particles with a density of 1000 kg/m^3 have approximate values: υ_g = 4 × 10-7 m/s for 0.1 μm particles and υ_g = 4 × 10-5 m/s for 1 μm particles. For 10 μm particles, the falling velocity is υ_g = 3 × 10-3 m/s, and for 100 μm particles υ_g = 3 × 10-1 m/s [4, 5]. On the other hand, SiO_2 silica grains with contractual diameters of d_p = 10, 50 and 100 μm and density of 2650 kg/m^3 fall with velocities of respectively: υ_g = 0.035, 0.11 and 0.72 m/s [6, 7].

The mass of dust (in grams or milligrams) found in 1 m^3 of ambient air is a measure of the dust content in the air. This parameter is defined as dust concentration, which is a variable quantity that depends on many factors. In the case of a moving vehicle, the dust concentration in its environment depends on the type of ground (sandy, loess), the speed of travel, the presence of other vehicles, weather conditions (rain, drought, wind direction), the type of chassis (wheeled, tracked). Therefore, the concentration of dust in the air is shaped in a wide range. The author of the paper [8] reports that the concentration of dust in the air takes insignificant values from 0.01 mg/m^3 near rural buildings to about 20 g/m^3, when driving a column of tracked vehicles over desert terrain. According to the author of the paper [9], dust concentrations in the air can take on values in a wide range of 0.001–10 g/m^3. Dust concentrations on highways take on small values, but in the wide range of 0.0004–0.1 g/m^3. Experimental studies presented in the paper [10] show that when a column of vehicles travels over sandy terrain, dust concentration takes on values in the range of 0.03–8 g/m^3.

Dust grains of silica SiO_2 and alumina Al_2O_3, whose mass content in the dust reaches 95%, are the main cause of accelerated abrasive wear of the two frictionally cooperating machine components when they enter the piston headspace. According to the hardness derived from the 10-grade Mohs scale, silica has a hardness of 7, and alumina has a hardness of 9. In the case of reciprocating internal combustion engines, the surfaces of the P-PR-C (piston – piston rings – cylinder walls) mating elements and the journal-pan (J-P) mating elements of the engine crankshaft are most prone to accelerated abrasive wear. Hard dust grains settle on the cylinder liner, and then, because of piston movement, penetrate between the ring and cylinder faces, where there is a layer of lubricating oil (lubricating wedge). In the mating of a modern internal combustion engine, the thickness of the oil film hmin between the two surfaces depends on the viscosity of the oil, the load (contact force) and the relative speed of the two surfaces and take values in the range h_{min} = 0.3-50 μm [11, 12]. The greatest wear of two frictionally cooperating machine surfaces is caused by dust particles dp, for which the condition is met at a given time: the diameter of dp is equal to the thickness of the oil film hmin. Therefore, abrasive wear of engine components is caused

by dust particles with diameters in the range of 1–40 μm [13–15] with the highest intensity of wear caused by mineral dust grains in the diameter range of 1–20 μm [16–18].

Excessive abrasive wear of the piston ring and cylinder liner assembly of an internal combustion engine has a significant impact on the loss of tightness of this association. This is a direct cause of the loss of compressed medium and a decrease in compression pressure, resulting in a decrease in engine power and an increase in fuel and oil consumption [19]. Excessive wear of the P-PR-C association is also the cause of increased exhaust gas blow-by into the crankcase, which reduces its viscosity, accelerates oil aging and causes soot contamination [20].

In order to reduce friction losses and wear on the main components of an internal combustion engine, antiwear coatings on the sliding surfaces of piston rings and cylinder faces are appropriate [21]. A significant reduction in frictional losses in an internal combustion engine can be achieved by ensuring continuity of the oil film by selecting the shape of the sliding surfaces of both the upper and lower sealing ring [22].

A device that ensures minimization of abrasive wear of engine components is an air filter installed in the intake system, which ensures that air of the required purity, i.e. free of dust grains larger than 2–5 μm, is supplied to the engine cylinders. Single-stage (baffle) filters are installed in the intake systems of passenger car engines that operate with low concentrations of dust in the air. Sufficient air cleanliness is then provided by a filter element made of pleated paper formed into a rectangular plate. Engines of trucks, special vehicles, including military vehicles, and work machines, which are most often used in conditions of high air dustiness, are equipped with two-stage filters operating in the «multicyclone-pore baffle» system [23, 24].

2. THE ORIGINS OF ENGINE INLET AIR FILTRATION

An air filter is a device that separates contaminants from liquids as a result of various forces and phenomena generally referred to as filtration mechanisms. Air filters differ in their operating principle, construction, type of filter materials used and the resulting operating parameters: filtration efficiency and accuracy, absorption capacity and pressure drop.

Baffle filters are currently the most popular group of air filters for motor vehicles and working machines. Baffle filters are used as single-stage filters in passenger cars or as the second stage of multi-stage filters used in the intake systems of vehicle engines operating in dusty air conditions. A variety of porous materials are used for filter baffles. They are called solids, which contain in their volume a large number of voids (pores), the characteristic dimension of which is small in comparison with the characteristic dimension of the solid [25]. The first stage of filtration in two-stage filters are inertia filters in the form of monocyclones or multicyclones, which are characterized by the separation of large dust masses from large air flows.

The first air filters that were used in engine intake systems were of a primitive form. In the 1901 Oldsmobile engine, the filter element was a baffle made of two layers of perforated sheet metal with holes 3 mm in diameter. In the 1901 Adler car, the filter baffle was a sleeve made of several layers of rolled metal mesh [26].

It was not until before World War II that work began to develop an air filtration system for the engine's intake system. An air filter in the form of a tin can with a filter baffle in the form of metal wadding moistened with oil was used, which increased filtration efficiency, which, however, did not exceed 70%. Cylindrical mesh filters saturated with oil with radial air inlets were characterized by relatively high absorption capacity and relatively low pressure drop (Figure 1 a). This type of design was used in motorcycles, among others (Fig. 1 b).

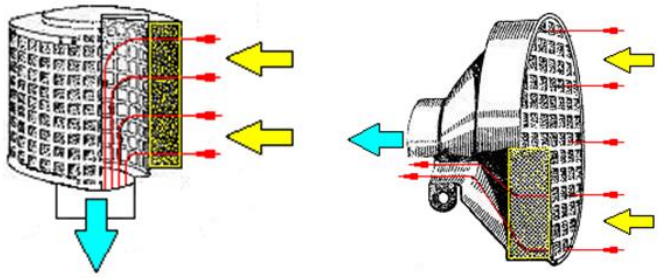

Figure 1. Filter with moistened metal mesh insert: a) automotive, b) motorbike [27]

In an improved design of this filter, the air flow was fed tangentially into a conical filter vessel partially filled with oil, which was swirled [27]. The oil swirling in the vessel rises along the surface of the cone and completely covers the air inlet opening to the filter. The intake air must pierce the wall of the swirling oil and is thus well mixed with it and cleaned of dust. The oil droplets entrained by the airflow are thrown by inertia against the vessel wall or settle on a baffle made of irregularly arranged and compressed metal wire or labyrinth plates (Fig. 2 a). An improvement to this method of air filtration was to dispense with passing the air through the oil and to bring it perpendicular to the oil mirror (Fig. 2 b) [28].

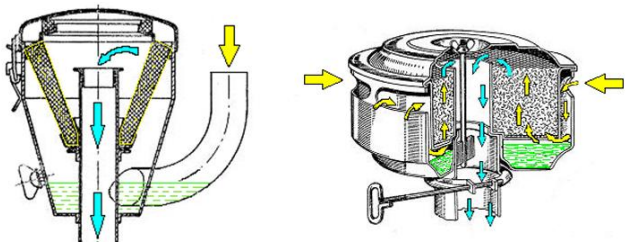

a b

Figure 2. Air filter with wet mesh bed and oil sump: a) swirled [27], b) flushed [28]

The incoming aerosol rapidly changes the direction of flow over the oil surface. Contaminants of the largest size and mass, as a result of the force of inertia, fall into the oil, where they are retained. Contaminants of smaller size and mass are retained by the humidified cartridge.

A breakthrough in air filtration for internal combustion engines did not occur until the early 1950s after the development of a special type of porous paper, which was used in place of a metal mesh baffle moistened with oil. In 1957, Knecht Filterwerke introduced and patented the pleated paper filter cartridges that are still known today, which are much simpler to use and, above all, lighter and cheaper. The pleating of the paper made it possible to use a large filter area with limited space for mounting the filter. This solution, in addition to the introduction of more and more perfect filter materials, such as polyester, fiberglass, nanofibers, is widely used to this day in the production of panel filter cartridges of passenger car filters and cylindrical cartridges that are the second stage of filtration of air filters of articulated cars, trucks and special vehicles.

3. SINGLE-STAGE AIR FILTRATION SYSTEM WITH FILTER PAPER

Air filters for passenger vehicle engines are installed in the engine compartment due to their small dimensions resulting from the low air demand of the engine and thus the small surface area of the filter paper. The shape of the filters is then adapted to

the limited space of this compartment. This ensures at the same time easy access during servicing, simple and easy installation of the filter element and other replacement elements, tightness of its connection to the intake manifold, minimum length of connecting lines. In older types of passenger cars, the air filter was seated directly on the carburettor, which was attached to the intake manifold. Due to the restriction of the engine bonnet, the filter was usually flattened in shape and the filter element was made in the form of a large diameter ring (Fig. 3). In addition, mounting the air filter on or close to the engine causes it to be subject to high vibrations, which adversely affects the filtration efficiency and its service life.

In modern passenger car models, the carburettor fuel system has been replaced by a fuel injection system, and therefore air filters can be mounted anywhere in the engine compartment away from the engine. Therefore, the filter is most often attached to the body, its housing is adapted in shape to the limited space of the engine compartment (Fig. 4).

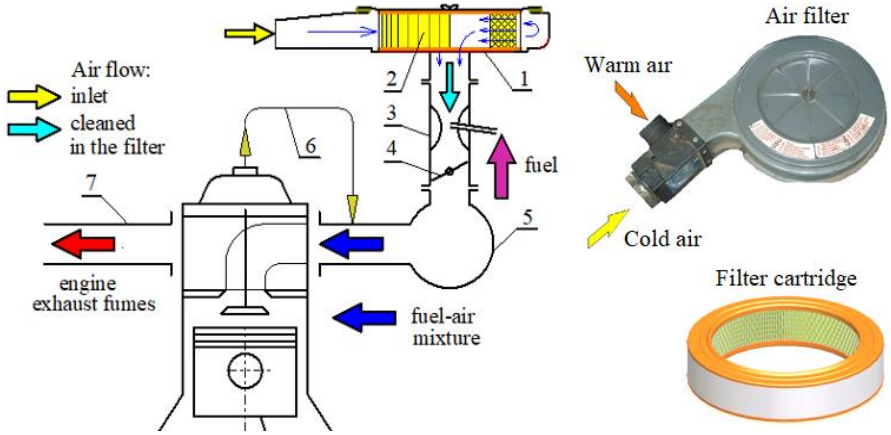

Figure 3. Intake air filtration system for an engine with a carburettor in a passenger car: a) functional diagram of the intake system (1 – air filter, 2 – filter cartridge, 3 – carburettor, 4 – throttle, 5 – intake manifold, 6 – crankcase ventilation system, 7 – exhaust manifold) b) view of the filter, c) ring filter cartridge with fiber pre-filter

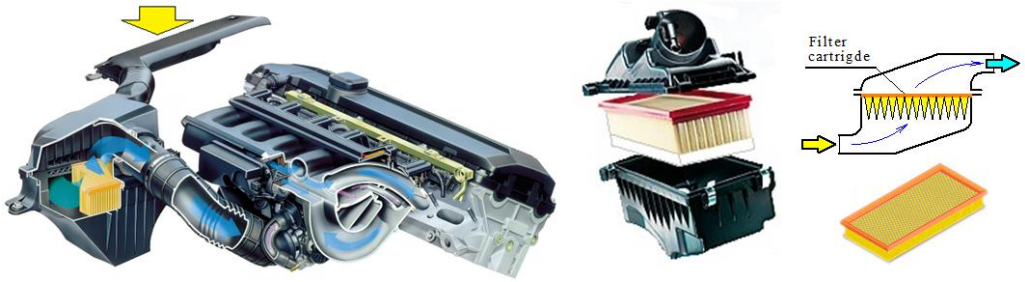

a b c

Figure 4. Air filter of a modern passenger car: a) location of the air filter in the engine compartment [29], b) components of the filter, c) functional diagram of a single-stage filter [30, 31]

The design of the air filter of a modern passenger car is not complicated. The filter housing is a two-part box, similar in shape to a cuboid, most often made of plastic. The housing is made of two covers, lower and upper, after disconnecting which it is possible to place a filter insert in the middle in the form of a panel made of pleated filter paper, composite or non-woven fabric (Fig. 4). The lower cover is connected to a pipe supplying ambient air from the front of the car. The upper cover is connected to a pipe discharging purified air to the intake manifold.

4. PROPERTIES OF FILTER MATERIALS

The basic filter material used for filtration of operating fluids of modern motor vehicle engines and working machines, and in particular for filtration of intake air of motor vehicle engines, are filter papers. They combine the operation of meshes and nonwoven fabrics.

To improve the properties of paper, it is impregnated with appropriate resins (saturation) and then hardened. This treatment increases the properties of paper, including mechanical strength, resistance to chemical compounds, oil and fuel, resistance to flammability and improves plasticity, as well as modify the color and reduces hygroscopicity. Paper hardening occurs in the process of producing filter inserts by heating it to a specific temperature after pleating the paper and giving it the shape of a filter insert and impregnating it with resin.

During curing, the filter paper changes color and texture, which is different on both sides. The sieve (bottom) side of the paper has smaller pore sizes than the top side. In the filter, the paper should be arranged so that the liquid flows in from the top side of the paper and out from the sieve side. To avoid confusion, the side of the paper is marked with colored lines during production.

Filter materials are characterized by the following basic parameters as stated by the manufacturer: basis weight, thickness, average pore size, fiber diameter, dirt absorbency, air permeability, tear strength, maximum or average pore diameter, resin content. Table 1 summaries the characteristic parameters of selected filter papers from J.C.Binzer. It is noteworthy that the thickness of the filter papers does not exceed 1 mm and is mostly in the range of 0.5–0.9 mm, with the diameter of the cellulose fibers taking d_w = 15-20 μm. The average pore diameter takes on values of d_r = 40-90 μm.

For the production of modern filter materials, plastics are increasingly used in addition to filter papers: glass microfibers, polyester, non-woven fabrics and nanofibers, which improves the filtering efficiency and filtration accuracy of filter cartridges and their durability. In addition, multilayer beds that are a composite of different materials, such as cellulose-polyester-nanofiber, cellulose-polyester, polyester-microfibre-glass-cellulose, are increasingly being used for intake air filtration in motor vehicle engines. Multilayer beds show a higher dust-absorbing capacity compared to single-layer configurations, allowing the air filter to be used longer until the limit of acceptable resistance is reached.

Table 1

Parameters of selected filter papers from J.C.Binzer [32]

	Parameters	Units	Paper designation			
			796/1 VH86	356 VH86/4	844 VH86/4	879 VH188/51
1	Grammage	g/m^2	204	125	108	139
2	Thickness – at load 2 N/cm^2	mm	0,9	0,61	0,67	0,8
3	Pressure drops, at: Q = 400 cm^3/s, A = 10 cm^2	mbar	6,7	1,5	1,04	0,66
4	Breaking strength	kPa	385	251	212	220
6	Resin content	%	18,8	18	17	20
7	Maximum value of pore diameter	μm	51	72	89	103
8	Average value of pore diameter	μm	42	62	76	93

Table 2 compares the characteristic parameters of selected filter materials. Of note is the significantly higher air permeability and twice the pore size of the filter paper (cellulose) compared to the other materials.

Table 2

Tested filtration materials parameters according to the manufacturer's data [33]

	Filtration material	Permeability q_p [m^3/m^2/h] at 200 Pa	Permeability q_p [dm^3/m^2/s]	Grammage g_m [g/m^2]	Thickness g_z [mm]	Max. pore size d_p [μm]
1	Cellulose	-	838	121	0.61	79
2	Poliester	650	-	180	0.50	-
3	Cellulose+polyester	-	150	130	0.35	58
4	Cellulose+polyester + nanofibers	-	185	120	0.31	48
5	Poliester+nanofibers	525	-	180	0.51	-

On the two standard filter materials (No. 4 and 5), there is a layer of nanofibers on the inlet side. The thickness of the multilayer filter beds is less than that of traditional filter papers and is mostly in the range of 0.3–0.6 mm, which is due to the smaller diameter of the plastic fibers.

Non-woven fabrics are also used for air filtration in motor vehicles and are characterized by [25]: loose structure, spatial packing, lightness, ease of fabrication high dirt absorbency, low pressure drop. However, synthetic nonwovens have very low rigidity and therefore the construction of traditional filter media is cumbersome. Therefore, rigid plastic frames are used to which a gasket is attached to ensure tightness with the filter housing. Some solutions use pleated fibers together with special plastic meshes.

Table 3 shows the characteristic parameters of selected filter nonwovens manufactured by a Korean company. The thickness of non-woven filter beds is several times greater than that of traditional filter papers or multilayer beds and is usually in the range of 2.5–4 mm.

Table 3

Properties of nonwoven filter fabrics manufactured by Korea Filtration Technologies Co [34]

Non-woven fabric	Grammage [g/m^2]	Thickness [mm]	Permeability [cm^3/cm^2/s]	Tensile strength [N/50 mm]	Bending strength [N/30 mm]	Bending strength [MPa]
AC-1800	290	2,8–3,6	50–85	>98	1,96–3,62	0,49
AC-3800	240	3,15–3,85	65–90	>98	1,96–3,62	0,39
AC-3421	230	2,43–2,97	55–70	>147	1,47–2,94	0,59
AC-303	250	2,7–3,3	75–95	>98	1,47–2,25	0,59
AC-301	210	2,43–2,86	80–110	>98	1,47–2,94	0,59
AC-510	205	2,7–3,3	90–140	>98	1,47–2,94	0,49

An image of the structure of the filter materials obtained by scanning electron microscopy is shown in Figure 6. The fibers represent the three-dimensional disordered spatial network structure of the polypropylene microfibre filter material (Figure 5 a) and cellulose (Figure 6 b).

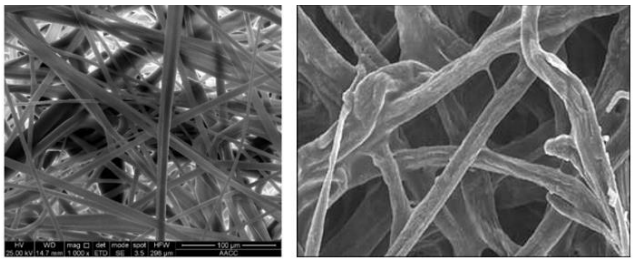

a b

Figure 5. SEM image of filter material:
a) polypropylene microfibre at 1000 magnification b) cellulose [35]

5. FILTRATION MECHANISMS

Dust particles flowing with air onto the filter bed are retained by individual fibres as a result of the simultaneous action of several filtration mechanisms: interception, inertial, diffusion, gravitational settling and sieving mechanisms [36, 37] (Fig. 6). The interception mechanism occurs when a particle follows the line of the air stream that flows around the bed fibre and comes into physical contact with it. The inertial mechanism applies to particles of large mass that cannot adapt to sudden changes in the direction of the air stream directly in front of the fibre. Due to their high inertia, the particles continue to move in a rectilinear path and therefore come into contact with the fibre, where they are retained. The inertial mechanism is more effective at high particle velocities [37]. On the other hand, the diffusion mechanism applies to small particles (<0.1 μm) and is effective in the case of their low velocities. Particles randomly performing Brownian motion collide with the fibers and settle there. The gravitational mechanism concerns particles of large size and mass, which settle on the fibers under the influence of gravity. However, the influence of gravity is negligible for particles smaller than 0.5 μm [33]. Dust particles with diameters larger than the distance between adjacent fibers are retained by the sieve mechanism. The filtration efficiency of the fibrous bed is the total result of the combined effect of all filtration mechanisms (Fig. 7). The graph shows that particles from 0.1 μm to 0.4 μm have the lowest retention efficiency. This characteristic range is called the most penetrating particle size (MPPS) and depends on the filtration speed and the fiber size [37, 38]. When the fiber is electrostatically charged, the particle capture efficiency additionally increases due to electrostatic attraction [39].

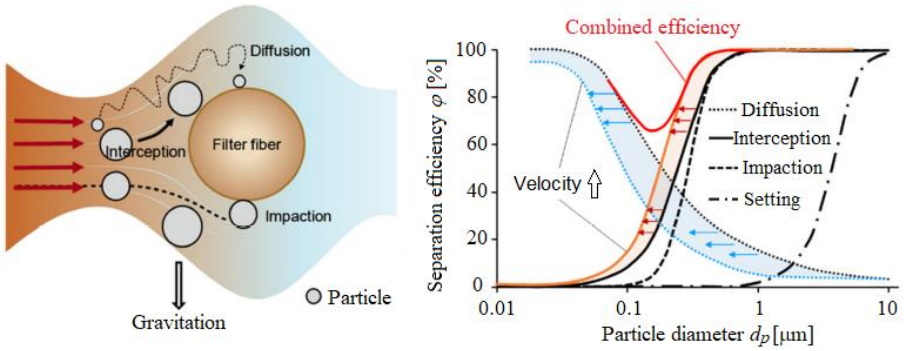

a b

Figure 6. Particle retention mechanisms. (a) particle retention by a single fiber: (b) combined effect of particle retention mechanisms on overall filtration efficiency [36]

The effect of the filtration mechanisms in the filter bed is that dust particles are retained on the surface of the porous bed fibers and then on the previously deposited particles. In this

way, slowly growing complex dendritic structures (agglomerates) are created, which fill the free spaces between the fibers (Fig. 7). This causes a change in the structure of the filter bed, as a result of which its operating parameters change.

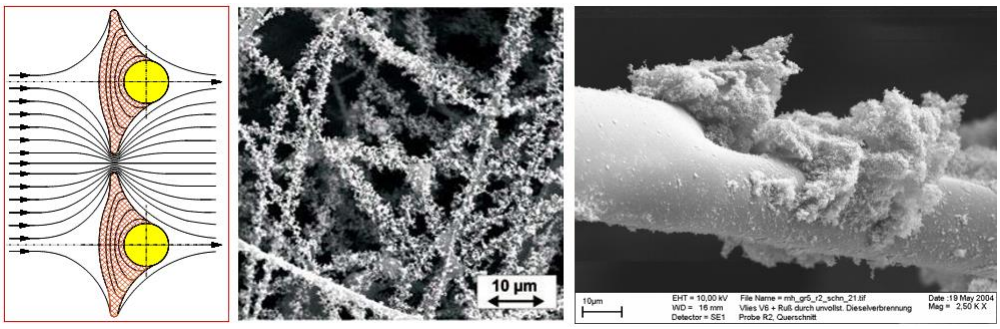

a b

Figure 7. Accumulation of dust particles on the filter bed fibers: a) scheme of growth of successive layers on the fibers, b) structure of the filter bed with visible agglomerates formed by dust grains settling on the fibers, b) view of agglomerates on a single fiber [40]

6. SHAPING TRADITIONAL FILTER MEDIA

Filter media intended for the filtration of operating fluids in motor vehicles are made in the form of a pleated tape, which is then shaped into a multi-armed star or a panel (Fig. 8). Cylindrical or panel filter elements are then obtained.

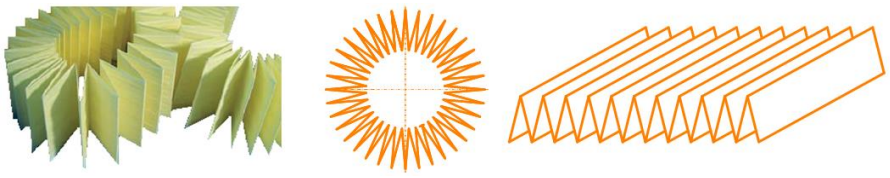

a b c

Figure 8. Shaping filter paper: a) paper after pleating, b) shaping into a multi-pointed star, c) shaping into a panel

The most common is the V-shaped pleat formation or, for better use of the insert space, the W-shaped pleat formation (Fig. 9). Pleated paper filter inserts should be designed in such a way that, with the given paper filtration parameters, they have maximum filtration efficiency, minimum pressure drop and maximum durability, and they should have maximum paper surface area with minimum insert volume. The air filter insert consists of a housing and a filter material placed inside it. The housing is made of polyurethane, which also acts as a seal for the filter material.

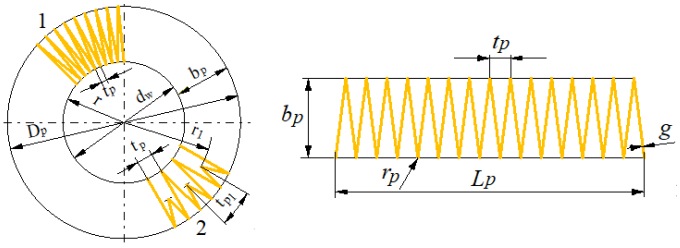

a b

Figure 9. Forming the pleats of filter paper: a) cylindrical insert (1 – V-shaped, 2 – W-shaped), b) panel insert, D_p – outer diameter of the cylindrical part, d_w – inner diameter of the cylindrical part, b_p – pleat height, t_p – pleat spacing, pitch, L_p – panel length, g – paper thickness, r_p – pleat bend radius

The covers (upper and lower) of the cylindrical insert made of polyurethane ensure a tight connection of the ends of the pleats with each other, creating space for the inflow of air and dust, and at the same time a tight connection of the insert with the filter housing. Reinforcing elements in the form of sheet metal or plastic mesh ensures the appropriate mechanical strength and stiffness of the insert and increases its resistance to the effect of the pressure difference (resistance to deformation) created during engine operation, and in particular when the insert is excessively contaminated. The construction of the panel insert is much less complicated. The ends of the shorter sides of every second pleat are glued together on both sides, creating space for the inflow of air and dust, and then at an appropriate distance t_p connected with a polyurethane frame, which is also a seal for the filter housing. The condition for the correct operation of the filter is the tightness between the filter insert and the filter housing.

The selection of an air filter for an engine consists in determining and using the appropriate filter paper surface area, which results from the condition of permissible filtration speed, which has been verified experimentally and takes the maximum value in the range of υ_{Fmax} = 0.08-0.12 m/s [41-44]. Filtration speed is defined as the average speed of the air flowing through the surface of the filter medium and is determined from the relationship:

$$\upsilon_{Fmax} = \frac{Q_{Fmax}}{A_c \cdot 3600} \text{ [m/s]}, \tag{1}$$

where: Q_{Fmax} – maximum air flow through the filter element equal to the air demand of the Q_{Silmax} engine [m^3/h] at the maximum power rotation speed and 100% opening of the mixture throttle (SI engines), A_c – active filter surface area of the element [m^2].

In modern passenger cars, there is a problem with the proper location of the air filter in the engine area – under the hood. There is no such problem in the case of trucks, where the air filter and the entire intake system are mounted outside the vehicle cabin. The smaller surface area of the filter paper results in an increase in the air flow speed through the filter bed, while maintaining the same air flow value. As a result, there is an increase in the air filter pressure drop, which is a function of the speed in the second power, which is a direct cause of the decrease in engine filling and power and an increase in exhaust emissions. Significantly exceeding the permissible speed may cause a decrease in filtration efficiency due to the phenomenon of dust particles bouncing off the surface of the bed fibers and being re-entrained by the air flow towards the outlet.

Obtaining the appropriate filtration speed is possible by appropriate selection of the main structural dimensions of the insert and the geometry of the pleats (Fig. 10) [43–45].

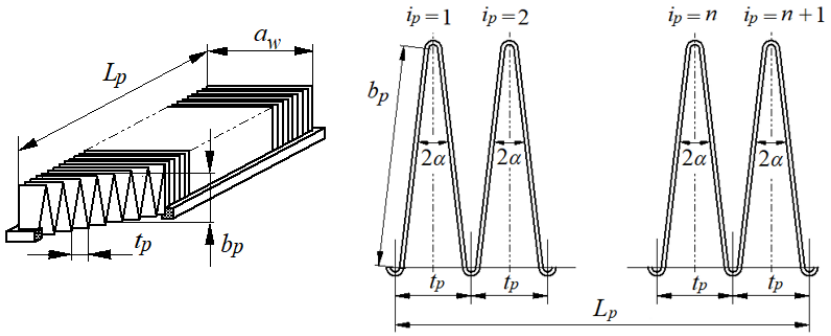

a b

Figure 10. Filter bed geometry: a) pleat geometry, b) i_p – number of pleats, Lp – insert length, a_w – pleat width, b_p – pleat side height, t_p – pleat width, α – half-pleat inclination angle

In the case of panel inserts, the filter surface of the insert is determined by its dimensions (Fig. 10), which are related to the relationship:

$$A_c = 2h_p \cdot a_w \cdot t_p \cdot i_p [m^2]. \quad (2)$$

The width of the insert aw and its length L_p are limited by the filter dimensions. A limited number of pleats can be placed at a given length L_p and with a fixed pleat spacing t_p. The filtration surface can be increased by extending the pleat side b_p, which will reduce the filtration speed and pressure drop, but only to a certain value, because pleats that are too high are unstable, warp and touch, causing a loss of filtration surface. The filtration surface can be increased by increasing the number of pleats in a given section, which will reduce the flow speed and reduce pressure drop, but here too there is also a certain limit on the number of pleats, exceeding which will increase pressure drop. The available literature contains a significant number of works presenting the results of optimization of filter beds and complete air filters, mainly in the direction of minimizing pressure drop or increasing filtration efficiency. These parameters determine the engine energy losses and accelerated wear of its components [46–50]. Examples of panel filter insert designs for passenger car engines made of various materials are shown in Figure 11. The edges of the insert are fitted to the lower and upper filter housings, acting as a seal at the same time.

a b c

Figure 11. Types of engine intake air filter inserts: a) paper filter inserts, b) non-woven fabric filter insert in a rigid frame, c) non-woven fabric filter insert made as a uniform moulding

Examples of the construction of cylindrical filter inserts which are the second stage in two-stage filters are shown in Figure 12.

a b c d e

Figure 12. Different solutions of filter cartridges working as a second stage after the inertia filter: a) cylindrical cartridge with an elliptical cross-section, b, c, d, e) cylindrical cartridge with a circular cross-section

During the operation of the insert, the paper filter bed fills with dust, which significantly impedes the high-speed air flow. There is a significant increase in pressure drop, and the external sign of this phenomenon is the contact and warping of the pleats. To prevent this phenomenon, pleat reinforcements are used in the form of embossing of the pleat surface, special thickenings of the pleat back (Fig. 4 a–b) and thin streams of glue connecting the pleat backs of the insert (Fig. 13 c).

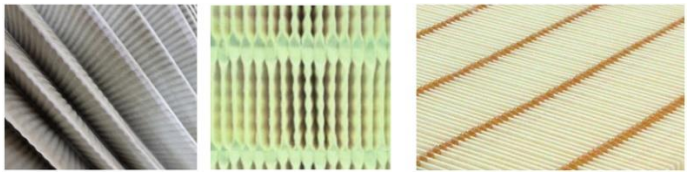

a b c

Figure 13. Methods of reinforcing pleats: a) embossing the pleat surface, b) special thickening of the back of the insert pleat, c) glue trickles

7. FORMING FILTER PARTITIONS WITH AXIAL FLOW

The lack of stability of the pleats, the need to reinforce them, and the need to meet the requirements of small dimensions while maintaining the required efficiency and accuracy of engine intake air filtration were the reasons for developing a different filter design and a new technology for making filter inserts. Their characteristic feature is the axial flow of the air stream. This allows to avoid turbulence and allows air and dust to flow directly to the filter outlet, which minimizes pressure drop. An example of such a solution is the filter insert known as PowerCore by Donaldson (Fig. 14). PowerCore filter inserts have a core structure created by alternating layers of smooth and corrugated paper. The channels created in this way are alternately plugged. If a given channel is free on the inlet side, it is blocked on the outlet side and vice versa. Such a design forces air to flow to the adjacent channel through the side surface, which is the filter material.

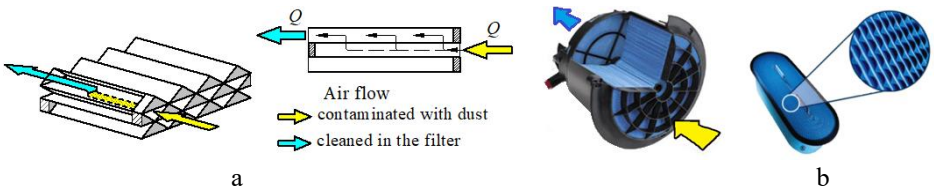

a b

Figure 14. PowerCore filter insert: a) principle of operation of the filter insert, b) air flow through the insert [51]

PowerCore filtration technology combines the axial filter model with nanofiber technology, which resulted in reduced volume and high filtration efficiency. At the same air flow rate, filters made with PowerCore technology are 2–3 times smaller in size than filters with pleated filter paper inserts made using the traditional method and more efficient (φ_f = 99.97%) than an average conventional filter achieving efficiency of (φ_f = 99.85% [52, 53].

The design of the PowerCore G2 insert allows for a 60% reduction in the size of the insert and a nearly three-fold increase in the dust absorption capacity of the filter inserts, compared to conventional solutions used so far, while maintaining the same constant surface area of the filter paper and constant dimensions of the insert (Fig. 15).

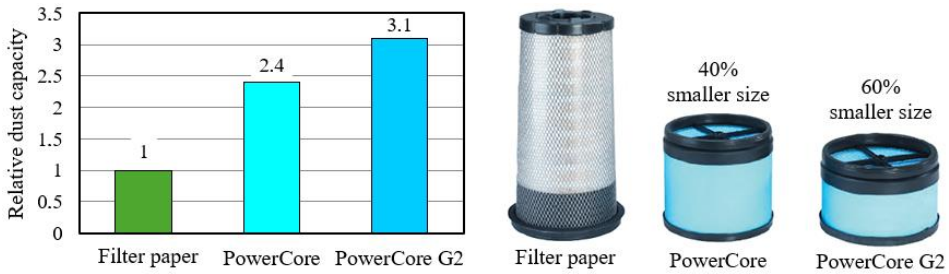

a b

Figure 15. Comparison of PowerCore cartridges with respect to traditional (filter paper) filter cartridge: a) relative dust capacity, b) occupied volume [54, 55]

Reducing the dimensions of the filter element entails the possibility of reducing the dimensions of the entire air filter. Thanks to their design, PowerCore filter elements are characterized by very high absorption capacity. More modern filter elements are elements made using PowerCore G2 technology, introduced into production in 2008. The essence of this technology is very precise shaping of the geometry of the filter core channels depending on the type of engine to which it is to be applied.

The axial air flow, allowing for flow directly to the filter outlet and minimizing aerosol pressure drop, is provided by the Direct Flow filter element manufactured by Cummins (Fig. 16 a), in which the channels are formed by traditional pleats alternately sealed on its shorter sides and shaped in the form of panels [42]. The filter element can be constructed in the form of a trapezoid made of two panel inserts set at a small angle (Fig. 16 a) or in the form of two coaxially set cylinders (Fig. 16 b). Such a design forces air to flow through the pleats from the front and along the longer sides and air to flow out on the opposite side.

a b

Figure 16. Principle of operation of the Direct Flow panel filter insert
a) air flow diagram, b) insert construction [56, 57]

The core insert manufacturing technology (PowerCore) was used by Baldwin in the Channel Flow filter (Fig. 17).

The PowerCore filter element allows for a reduction of the filter space by up to 50% compared to traditional cylindrical filters. The same technology used by Mann+Hummel in the PicoFlex filter has resulted in the CompacPlus filter element having 50% more filter media surface than a conventional air filter.

a b c

Figure 17. Filter inserts made with modern technologies: a) traditional PowerCore (Donaldson) [13], b) CompacPlus (Mann+Hummel) [58], c) Channel Flow (Baldwin) [59]

Despite the obvious advantages that PowerCore filters have compared to traditional cylindrical elements, they are not yet widely used for engine intake air filtration due to the significant (several times higher) cost.

8. PROPERTIES OF NANOFIBER FILTER MATERIALS

The technological possibilities of fiber production have resulted in nanofibers being increasingly used to build filter partitions in automotive technology. The term nanofibers

usually refer to fibers with a diameter of less than 1 μm and are currently used for fibers produced using «electrospinning» or meltblown technology [60–65]. Currently, automotive technology uses nanofibers with diameters of about 50–500 nm, and the nanofiber layer does not exceed a thickness of 1–5 μm. Due to the low mechanical and strength properties of such a thin layer, it is applied to a substrate made of conventional filter materials (cellulose, nylon or polyester), which are thicker and stronger. Nanofibers can be placed on one or both sides of the filter bed. Fig. 25 a shows the view of the nanofiber material (d_{wl} = 0.15 μm) under an electron microscope at 1000x magnification in comparison to a human hair (d_w = 50-70 μm) and a cellulose substrate fiber (d_c = 10 μm) [66].

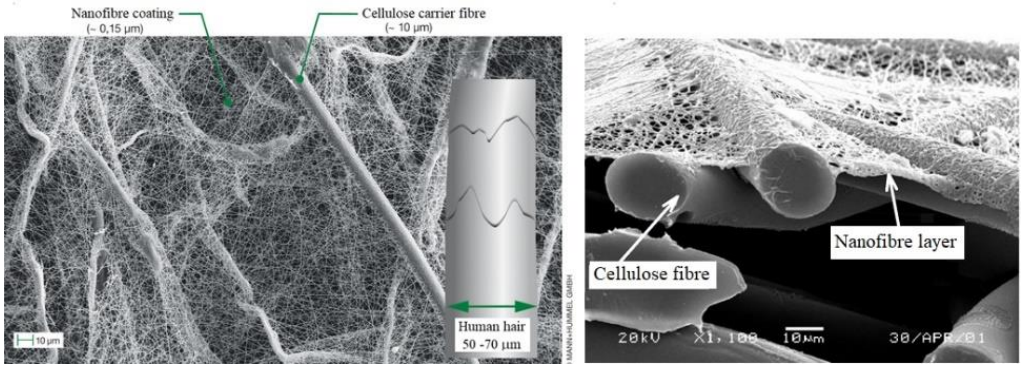

Figure 18. Nanofibers applied to a cellulose substrate:
a) top view [66], cross-sectional view [60]

The use of nanofibers as an additional layer applied to standard filter materials for air filters used in motor vehicles significantly improves filtration efficiency and accuracy, especially of dust grains of small (less than 5 μm) size. Figure 19 shows a clean cellulose bed with an applied layer of nanofibers with diameters in the range of 100–400 nm and a view of the retained dust grains on the bed.

Figure 20 shows the changes in filtration efficiency depending on the size of dust grains for a standard bed (made of cellulose fibers) and a cellulose bed with an additional layer of nanofibers. The increase in the filtration efficiency of dust grains below 5 μm is very visible. Grains of this size cause abrasive wear of engine components. For dust grains below d_p = 3.5 μm, the filtration efficiency increased from φ = 75.15% to 97% for the bed with a layer of nanofibers. For dust grains below d_p = 1.5 μm, the filtration efficiency increased significantly from φ = 29.2% to 82.1%.

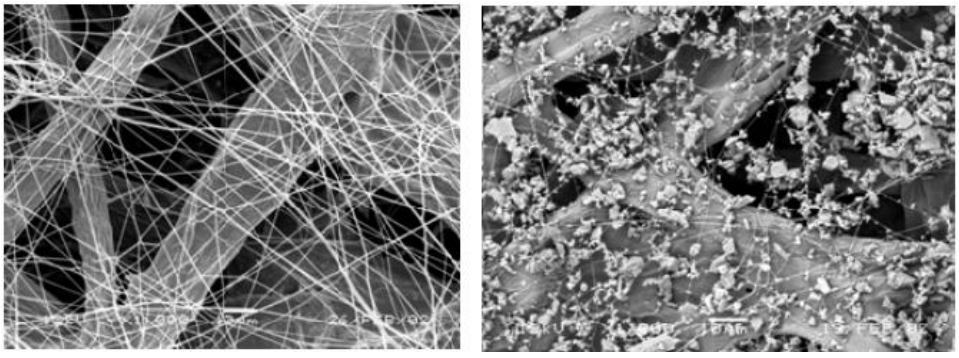

a b

Figure 19. nanofibers on cellulose substrate:
a) clean bed, b) dust cake on nanofiber layer [67]

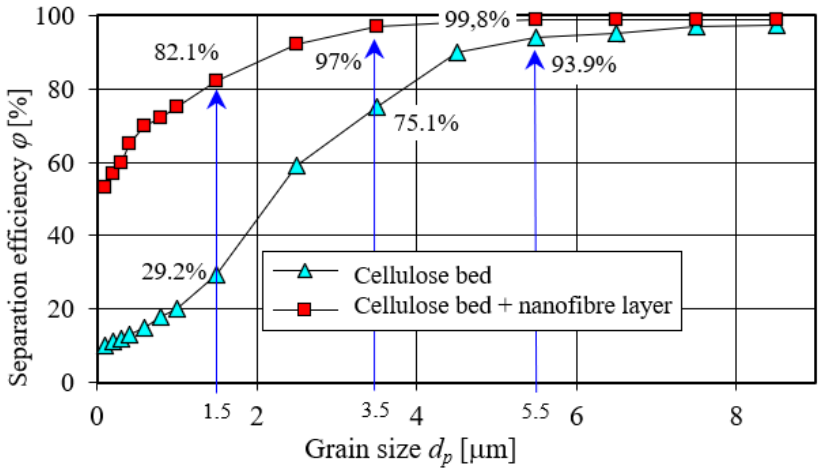

Figure 20. Separation efficiency as a function of dust grain size for a cellulose fiber bed (standard) and a bed with the addition of nanofibers [68]

9. EXPERIMENTAL TESTS OF FILTER DEPOSITS

The efficiency of the filter bed is described by the following filtration characteristics [25]:

- separation efficiency – φ_f,
- filtration accuracy – d_{pmax},
- dust absorption capacity – k_m,
- pressure drop – Δp_f.

Filtration efficiency φ_f, is defined as the quotient of the mass m_z of dust retained by the filter bed and the mass m_D of dust supplied to the bed in the air stream per unit of time.

$$\varphi_f = \frac{m_z}{m_D} 100\% \tag{3}$$

Filtration accuracy is defined as the maximum size d_{pmax} of dust grains in the air behind the filter bed.

The absorbency of the filter material is the mass of dust k_m retained on a unit of surface until the filter bed reaches the established operating conditions, e.g.:

- decrease in filtration efficiency or accuracy below the established value,
- achievement by the filter bed of a specified permissible pressure drop value.

Pressure drop is defined as the difference in static pressure p_{c1} before and p_{c2} after the filter:

$$\Delta p_f = p_{s1} - p_{s2} \text{ [Pa]} \tag{4}$$

The characteristics of filter beds (barrier filters) depend on many parameters. These are the parameters of dust, air flow, filter bed structure and bed operating conditions. For a specific air filter design and the associated filter bed, which operates within a fixed range of air flow values Q_{min}-Q_{max} and assuming constant parameters of atmospheric air and dust, the characteristics of a barrier air filter of a motor vehicle engine depend mainly on:

- m_p – mass of dust retained on the porous barrier,
- Q_F – air flow through the filter.

For practical purposes, the characteristics of air filters are determined as a function of one parameter, with the others determined, in laboratory conditions on special stands using standard research tests and using test dust. The following characteristics are most often performed for barrier filters:

$$\varphi_f = f(m_p) \text{ or } \varphi_f = f(k_m), \tag{5}$$

$$\Delta p_f = f(m_p) \text{ or } \Delta p_f = f(k_m), \tag{6}$$

$$d_{pmax} = f(m_p) \text{ or } d_{pmax} = f(k_m), \tag{7}$$

$$\Delta p_f = f(Q_F) \text{ or } \Delta p_f = f(\upsilon_F), \tag{8}$$

where: k_m – the dust absorption coefficient of the porous baffle is defined as the quotient of the dust mass m_p retained by the filter media and the active surface area of the filter media paper A_c, d_{pmax} – maximum grain size in the air behind the filter, υ_F – filtration speed.

Figure 21 shows examples of filter paper characteristics determined by the authors during laboratory tests: filtration efficiency $\varphi_w = f(k_m)$, filtration accuracy $d_{pmax} = f(k_m)$ and pressure drop $\Delta p_w = f(k_m)$ as a function of the dust absorption coefficient of the partition k_m.

The filter paper was shaped into a small cylindrical filter element with an active surface area of the filter material A_c = 0,148 m^2 and was conventionally called a «research filter». The characteristics were determined simultaneously on a special test stand for a constant air flow rate Q_F = 35 m^3/h, which corresponds to the filtration speed (υ_F = 0.065 m/s. Filtration efficiency $\varphi_w = f(k_m)$,was determined using the mass method for a constant air flow rate in subsequent j measurement cycles, during which the mass of dust fed to the filter and the mass of dust retained on the tested filter cartridge were measured. An absolute filter was mounted in the outlet air stream from the tested filter, which was used to perform mass balance during a single measurement. The absolute filter also protected against the inflow of dust particles onto the flowmeter sensor. The duration of the measurement cycle (time of uniform dosing of dust to the tested filter) was set at τ_{pd} = 2 min. in the initial period and τ_{pd} = 4-5 min. in the main period of operation of the filter elements. Before the planned end of the measurement (approx. 60 s), the procedure for measuring the number and size of dust grains in the air behind the filter was started at the particle counter. During the tests, PTC-D test dust was used, which is the equivalent of Arizona Fine dust with a maximum grain size d_{pmax} = 80 μm. After each measurement cycle, the necessary parameters were recorded, thanks to which the following were calculated.

After each measurement cycle, the necessary parameters were recorded, thanks to which the following were calculated:

- filtration efficiency using the relationship (3).

$$\varphi_j = \frac{m_{Fj}}{m_{Dj}} = \frac{m_{Fj}}{m_{Fj} + m_{Aj}} 100\%. \tag{9}$$

- dust absorption coefficient k_{mj} of the filter material:

$$k_{mj} = \frac{\sum_{j=1}^{n} m_{Fj}}{A_w} \text{ [g/ m}^2\text{]}. \tag{10}$$

- filtration accuracy as the largest dust grain diameter $d_{pj} = d_{pmax}$ that was recorded by the particle counter in the air stream Q_f behind the filter.

- pressure drop Δp_{ff} of the filter as the static pressure drop before and after the filter.

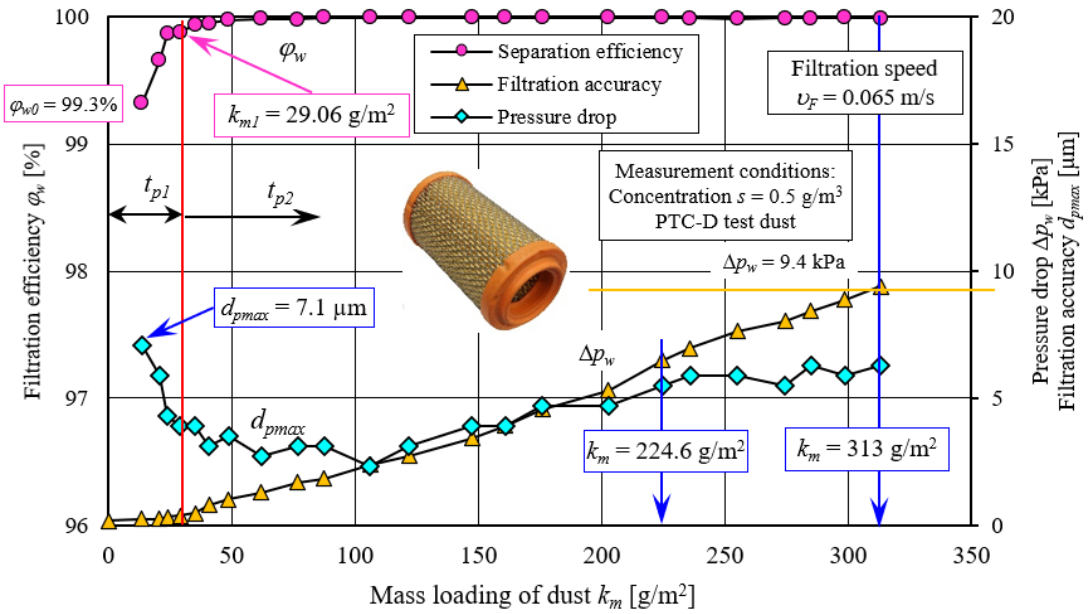

Figure 21. Characteristics of separation efficiency $\varphi_f = f(k_m)$ and filtration accuracy $d_{pmax} = f(k_m)$ and pressure drop $\Delta p_f = f(k_m)$ as a function of the dust absorption coefficient of the porous baffle k_m

The operation of the tested filter bed was conventionally divided into two stages (Fig. 21). It was assumed that the first (t_{p1}), the initial stage of the filter bed operation, lasts from the start of dust dosing until the filtration efficiency of φ_w = 99.5% is achieved. This stage is characterized by low initial efficiency and filtration accuracy (large dust grain sizes dpmax) and low pressure drop. In the initial filtration period, the filtration efficiency values take on low values (99.3%), which systematically increase with the amount of dust mass retained by the filter bed. The dust absorption coefficient km also increases, which for φ_w = 99.5% reaches the value k_m = 29.02 g/m^2. After the filter material reaches the set filtration efficiency value (φ_w = 99.5%), the second period of the filter bed operation (t_{p2}) begins, which is characterized by stable efficiency in the range (φ_w = 99.5-99.9%). During the initial filtration period, there are dust grains of considerable size d_{pmax} = 7.1 µm in the air behind the filter. When the filtration efficiency of φ_w = 99.5% is reached, the grain sizes decrease to the range of d_{pmax} = 2.7-3.9 µm. The pressure drop of the tested filter bed increases systematically with the amount of dust mass retained on the filter bed, which is consistent with the theory of filtration in fibrous beds. The maximum pressure drop of Δp_w= 9.4 kPa was obtained at a dust absorption coefficient of k_m = 313 g/m^2. After reaching the value of k_m = 224.6 g/m^2, dust grains above d_{pmax} = 5 µm appear in the air stream. In accordance with the requirements for filter papers, filtration accuracy above 5 µm eliminates the filter paper from further use. The initial period described by the value of the coefficient k_m = 29.02 g/m^2 constitutes approximately 12% of the efficient operation of the tested filter bed.

The phenomenon of low filtration efficiency and the presence of large (above d_{pmax} = 5 µm) dust grains occur at the beginning of the filtration process in a new filter bed, i.e. after each replacement of the filter element with a new one. Large dust grains can cause excessive abrasive wear of engine components. Therefore, work is being carried out to shorten the initial period, which is associated with the use of more effective filter materials.

Figure 22 shows the results of tests of filtration characteristics: filtration efficiency $\varphi_f = f(k_m)$, filtration accuracy $d_{pmax} = f(k_m)$ and pressure drop $\Delta p_f = f(k_m)$ as a function of the dust absorption coefficient of the partition km of three filter beds, including two composite fibers. The following variants of filter beds were tested, from which cylindrical filter inserts were made C (cellulose–polyester–nanofibers), D (cellulose–polyester), E (polyester). The materials were selected due to their distinct properties and known structural parameters. The tests were performed on the same stand using the same methodology.

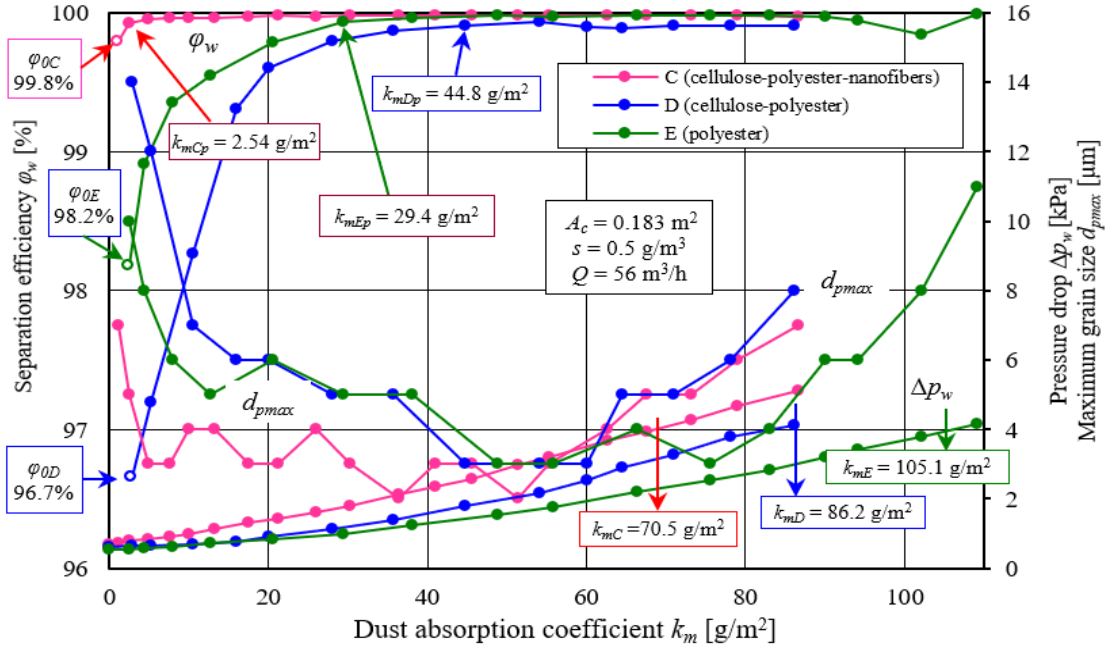

Figure 22. Comparative analysis of the characteristics of efficiency φ_w and filtration accuracy d_{pmax} and pressure drop Δp_w as a function of the dust absorption coefficient k_m of the filter media tested: C (80% cellulose-20% polyester-nanofibers, D (cellulose-polyester) and E (polyester)

The obtained characteristics of the filter inserts are similar in terms of the course but depending on the type of filter medium they are made of, they differ in value. The increase in the mass of dust collected in the filter layer is equivalent to an increase in the dust absorption coefficient km. In addition, there is an increase in the efficiency and accuracy of filtration, as well as in the pressure drop of the tested filter beds. This is characteristic of fibrous beds, but the increase in filtration parameters in the initial period is more intensive and changes in value for each insert. This results from the different properties (parameters) of the filter materials, such as permeability, thickness and grammage of the bed and the size of the pores. Particularly large differences in the course of the characteristics of the tested materials were recorded in the initial period of filtration, which lasts until the conventional efficiency of φ_w = 99.9% is achieved. The longest initial period was obtained by material D (cellulose-polyester), and the shortest by filter bed C (cellulose-polyester-nanofibers). The dust absorption coefficient assumes the values of k_{mDp} = 44.8 g/m² and k_{mCp} = 2.54 g/m², respectively. This means that the filter bed with a nanofiber layer effectively separates contaminants, and the outlet air from the filter contains dust grains below d_{pmax} = 7 µm. For comparison, the outlet air from the «D» filter contains dust grains below d_{pmax} = 14 µm, i.e. twice as large, which can cause accelerated engine wear.

10. CONCLUSIONS

1. The main component of road dust is silica (SiO_2) and alumina Al_2O_3, the proportion of which in the dust reaches 60–95%, and their hardness, assessed on the basis of the Mohs 10-point scale, has a value of 7 and 9, respectively, which far exceeds the hardness of structural materials used in engine construction and is the cause of accelerated wear, reduced reliability and engine life.

2. The greatest wear of two frictionally cooperating engine components is caused by dust grains in the 5–20 μm range. It is assumed that all mineral dust grains above 1 μm should be removed from the engine inlet air.

3. The predominant filter material of engine inlet air is filter papers, which show insufficient filtration accuracy of dust grains below 5 μm, hence the need to study other materials (fiberglass, polyester, nanofibers) in this area.

4. A characteristic feature of the process of aerosol filtration in filter materials is the occurrence of an initial period, which is characterized by low efficiency φw and filtration accuracy d_{pmax}, as well as low pressure drop Δp_w. In the air behind the filter cartridge there may then be dust grains of large size (14 μm), which cause accelerated wear of engine components, especially the piston, piston rings and cylinder, and as a result reduce its service life.

5. The duration of the initial filtration period (time until the required value of filtration efficiency φ = 99.9%.) varies and depends on the type of filter material. A layer of nanofibers applied to a substrate of conventional filter materials (cellulose, polyester) significantly increases the efficiency φ_w and filtration accuracy dpmax. Thus, the initial filtration period is several times shorter than a cartridge made of standard filter material. This has a definite effect on reducing the wear of engine components.

6. Filter cartridges made by PowerCore technology, while maintaining the same surface area of filter material, are dimensionally 2–3 times smaller than a cartridge made of pleated filter paper made by a conventional method and more effective in terms of filtration efficiency and accuracy than an average conventional filter.

References

1. Bojdo N., Filippone A. Effect of desert particulate composition on helicopter engine degradation rate, 40th European Rotorcraft Forum, Southampton, Conference Paper. September 2014.
2. Smialek J. L., Archer F. A., Garlick R. G. Turbine Airfoil Degradation in the Persian Gulf War. The Journal of The Minerals. Metals & Materials Society (TMS) 1994, 46 (12), pp. 39–41. https://doi.org/10.1007/BF03222663
3. Thomas G. E., Culbert R. M. Ingested Dust, Filters, and Diesel Engine Ring Wear. Society Of Automotive Engineers, Inc. West Coast Meeting San Francisco, Calif. August 12–15, 1968. https://doi.org/10.4271/680536
4. Wei-Han Su. Dust and atmospheric aerosol. Resources, Conservation and Recycling 1996, 16, pp. 1–14. https://doi.org/10.1016/0921-3449(95)00045-3
5. Juda J., Nowicki M. Urządzenia odpylające. PWN: Warszawa, 1986. (In Polish).
6. Dziubak T. Experimental Investigation of Possibilities to Improve Filtration Efficiency of Tangential Inlet Return Cyclones by Modification of Their Design. Energies 2022, 15, 3871. https://doi.org/10.3390/en15113871
7. Dzierżanowski P., Kordziński W., Otyś J., Szczeciński S., Wiatrek R. Napędy Lotnicze. Turbinowe silniki śmigłowe i śmigłowcowe; WKŁ:Warszawa, Poland, 1985. (In Polish)
8. Schaeffer J. W., Olson L. M. Air Filtration Media for Transportation Applications. Filtr. Sep. 1998, 35, pp. 124–129. https://doi.org/10.1016/S0015-1882(97)80292-3
9. Jaroszczyk T., Pardue B. A., Heckel S. P., Kallsen K. J. Engine air cleaner filtration performance – Theoretical and experimental background of testing. In Proceedings of the AFS Fourteenth Annual Technical Conference and 10. Exposition, Tampa, FL, USA, 1 May 2001.
10. Barbolini M., Di Pauli F., Traina M. Simulation der luftfiltration zur auslegung von filterelementen. MTZ – Motortechnische Zeitschrift, 2014, 5, pp. 52–57. https://doi.org/10.1007/s35146-014-0556-5

11. Barris M. A. Total Filtration™: The Influence of Filter Selection on Engine Wear, Emissions, and Performance. SAE Technical Paper 952557. Fuels & Lubricants Meeting & Exposition Toronto: Toronto, ON, Canada, Ontario, October 16–19, 1995. ttps://doi.org/10.4271/952557
12. Jaroszczyk T., Fallon S. L., Liu Z. G., Heckel S. P. Development of a Method to Measure Engine Air Cleaner Fractional Efficiency. SAE Trans, 1999, 108, pp. 9–18. https://doi.org/10.4271/1999-01-0002
13. Alfadhli A., Alazemi A., Khorshid E. Numerical minimisation of abrasive-dust wear in internal combustion engines. International Journal of Surface Science and Engineering, 2020, 14 (1), pp. 68–88. https://doi.org/10.1504/IJSURFSE.2020.105891
14. Bojdo N., Filippone A. Effect of desert particulate composition on helicopter engine degradation rate, 40th European Rotorcraft Forum, Southampton, Conference Paper. September 2014.
15. Long J., Tang M., Sun Z., Liang Y., Hu J. Dust Loading Performance of a Novel Submicro-Fiber Composite Filter Medium for Engine. Materials 2018. 11 (10). 2038. https://doi.org/10.3390/ma11102038
16. Nagy J. Filtration and engine life. Combust. Engines, 1973, 3, pp. 43–47.
17. Wróblewski P., Koszalka G. An Experimental Study on Frictional Losses of Coated Piston Rings with Symmetric and Asymmetric Geometry. SAE Int. J. Engines, 2021, 14, pp. 853–866. https://doi.org/10.4271/03-14-06-0051
18. Dziubak T., Dziubak S. D. A Study on the Effect of Inlet Air Pollution on the Engine Component Wear and Operation. Energies 2022, 15, 1182. https://doi.org/10.3390/en15031182
19. Woś P., Michalski J. Effect of Initial Cylinder Liner Honing Surface Roughness on Aircraft Piston Engine Performances. Tribology Letters, 2011, 41 (3), pp. 555–567, doi:10.1007/s11249-010-9733-y. https://doi.org/10.1007/s11249-010-9733-y
20. Koszałka G., Suchecki A. Changes in performance and wear of small diesel engine during durability test // Combustion Engines 2015, 162 (3), pp. 34–40. https://doi.org/10.19206/CE-116863
21. Wróblewski P., Rogólski R. Experimental Analysis of the Influence of the Application of TiN, TiAlN, CrN and DLC1 Coatings on the Friction Losses in an Aviation Internal Combustion Engine Intended for the Propulsion of Ultralight Aircraft. Materials 2021, 14, 6839. https://doi.org/10.3390/ma14226839
22. Wróblewski P. Effect of asymmetric elliptical shapes of the sealing ring sliding surface on the main parameters of the oil film. Combustion Engines. 2017, 168 (1), pp. 84–93. https://doi.org/10.19206/CE-2017-114
23. Dziubak T. Experimental Studies of Dust Suction Irregularity from Multi-Cyclone Dust Collector of Two-Stage Air Filter. Energies 2021, 14 (12), 3577. https://doi.org/10.3390/en14123577
24. Rieger M., Hettkamp P., Löhl T., Madeira P. M. P. Effcient engine air filter for tight installation spaces. ATZ Heavy Duty Worldw, 2019, 02. https://doi.org/10.1007/s41321-019-0023-9
25. Dziubak T. Filtracja powietrza wlotowego do silników spalinowych pojazdów mechanicznych. WAT Warszawa 2012. (In Polish).
26. Filtracja i filtry w pojazdach. AUTO-Technika Motoryzacyjna, nr 4, 1998. (In Polish).
27. Motyliński S. Poradnik mechanika samochodowego. PWT, Warszawa 1955. (in Polish).
28. Kordziński C., Środulski T. Układy dolotowe silników spalinowych. WKiŁ, Warszawa 1968. (In Polish).
29. Enderich A., Handel R. Mündungsschallprognose mit der Finiten Elemente Methode. MTZ Motortechnische Zeitschrift 60 1999, 1. https://doi.org/10.1007/BF03226488
30. Fleck S., Heim M., Beck A., Moser N., Durst M. Realitätsnahe Prüfung von Motoransaugluftfiltern. MTZ 2009, Jahrgang 70. https://doi.org/10.1007/BF03225494
31. Materiały informacyjne firmy WIX Filtron. Gostyń 2012.
32. Dziubak T. Analiza procesu filtracji powietrza wlotowego do silników pojazdów specjalnych. WAT Warszawa 2008.
33. Dziubak T, Dziubak S. D. Experimental Study of Filtration Materials Used in the Car Air Intake. Materials 2020, 13 (16), 3498. https://doi.org/10.3390/ma13163498
34. Dziubak T., Szwedkowicz S. Operating properties of non-woven fabric panel filters for internal combustion engine inlet air in single and two-stage filtration systems. Eksploatacja i Niezawodnosc – Maintenance and Reliability 2015, 17 (4), pp. 519–527. https://doi.org/10.17531/ein.2015.4.6
35. Teng G., Shi G., Zhu J., Qi J. (2023) A numerical simulation method for pressure drop and normal air velocity of pleated filters during dust loading. PLoS ONE 18 (2): e0282026. https://doi.org/10.1371/journal.pone.0282026
36. Jung S., Jooyoun Kim J. Advanced Design of Fiber-Based Particulate Filters: Materials, Morphology, and Construction of Fibrous Assembly. Polymers 2020, 12, 1714. https://doi.org/10.3390/polym12081714
37. Zhu M., et al. Electrospun Nanofibers Membranes for Effective Air Filtration. Macromol. Mater. Eng. 2017, 302, 1600353. https://doi.org/10.1002/mame.201600353
38. Bai H., et al. Theoretical Model of Single Fiber Efficiency and the Effect of Microstructure on Fibrous Filtration Performance: A Review. Ind. Eng. Chem. Res, 2021, 60, pp. 3–36. https://doi.org/10.1021/acs.iecr.0c04400

39. Ardkapan S. R., Johnson M. S., Yazdi S., Afshari A., Bergsøe N. C. Filtration E_ciency of an Electrostatic Fibrous Filter: Studying Filtration Dependency on Ultrafine Particle Exposure and Composition. J. Aerosol Sci, 2014, 72, pp. 14–20. https://doi.org/10.1016/j.jaerosci.2014.02.002
40. Trautmann P. Durst M., Pelz A., Moser N. High Performance Nanofibre Coated Filter Media for Engine Intake Air Filtration. AFS 2005 Conference and Expo, April 10–13, 2005.
41. Bugli N. Automotive Engine Air Cleaners - Performance Trends. SAE Technical Paper 2001-01-1356. https://doi.org/10.4271/2001-01-1356
42. Durst M., Klein G., Moser N. Filtration in Fahrzeugen, Mann+Hummel GMBH, Ludwigsburg, Germany 2005.
43. Erdmannsdörfer H. Lesttingmoglichkeiten von Papierfiltern zur Reinigung der Ansaugluft von Diselmotoren. MTZ 1971, 32, pp. 123–131.
44. Taufkirch G., Mayr G. Papierluftfilter für Motoren in Nutzfahrzeugen. MTZ 1984, 45 (3), pp. 95–105.
45. Gao J., et al. The Relationship between the Resistance Characteristics and Structural Parameters of the Elongated Filter Cartridge in the Dust Collector. Energy and Built Environment. Available online 1 April 2024. https://doi.org/10.1016/j.enbenv.2024.03.008
46. Allam S., Elsaid A. M. Parametric study on vehicle fuel economy and optimization criteria of the pleated air filter designs to improve the performance of an I.C diesel engine: Experimental and CFD approaches. Separation and Purification Technology 2020,. 241, 116680. https://doi.org/10.1016/j.seppur.2020.116680
47. Shi B., Yu X., Pu Y., Wang D. A theoretical study on the filtration efficiency and dust holding performance of pleated air filters. Heliyon 2023, 9, 7944. https://doi.org/10.2139/ssrn.4426974
48. Maddinenia A. K., Dasa D., Damodaran R. M. Numerical investigation of pressure and flow characteristics of pleated air filter system for automotive engine intake application. Separation and Purification Technology 2019, 212, pp. 126–134. https://doi.org/10.1016/j.seppur.2018.11.014
49. Kang S., Bock N., Swanson J., Pui D. Y. H. Characterization of pleated filter media using particle image velocimetry. Sep Purif Technol, 2020, 237, 116333. https://doi.org/10.1016/j.seppur.2019.116333
50. Saleh A. M., Fotovati S., Vahedi Tafreshi H., Pourdeyhimi B. Modeling service life of pleated filters exposed to poly-dispersed aerosols. Powder Technol, 2014, 266, pp. 79–89. https://doi.org/10.1016/j.powtec.2014.06.011
51. Genuine PowerCore® Air Filter Technology. Available at https://www.donaldson.com/content/dam/donaldson/engine-hydraulics-bulk/literature/north-america/air/f111632-eng/Genuine-PowerCore.pdf (accessed: 23 September 2024).
52. PowerCore®. Available at https://www.donaldson.com/pl-pl/engine/filters/products/air-intake/replacement-filters/powercore-filters/ (accessed: 23 September 2024).
53. Engine Air Filtration for Light, Medium, & Heavy Dust Conditions. Available at: https://www.donaldson.com/content/dam/donaldson/engine-hydraulics-bulk/catalogs/air-intake/north-america/F110027-ENG/Air-Intake-Systems-Product-Guide.pdf (accessed: 17 September 2022).
54. PowerCore® G2 and Ultra-Web® Filtration Technology. Available at: https://www.donaldsonaerospace-defense.com/library/files/documents/pdfs/059806.pdf (accessed: 23 September 2024).
55. PowerCore® G2 Filtration Technology for Engine Air Intake Systems. Available at: https://www. donaldson.com/content/dam/donaldson/engine-hydraulics-bulk/catalogs/air-intake/emea/f116005/Air-Intake-Product-Guide.pdf (accessed: 23 September 2024).
56. Fleetguard Direct Flow™. Available at: https://boschrexroth.africa/public/front_end/pdfs/products/d87431247a985c8500a37deb4796d719.pdf (accessed: 23 September 2024).
57. Mann+Hummel PicoFlex® The New Compact Air Cleaner for Highest Requirements. Available at: http://www.airnowsupply.com/BACKUP/catalogs/M+H%20PICOFLEX%20BROCHURE.PDF (accessed: 23 September 2024).
58. Baldwin's Channel Flow Air Filters. Available at: https://www.baldwinfiltersrus.com/media/baldwin-filters-pdf/channel.pdf (accessed: 23 September 2024).
59. Nanofibres are nanoscale materials. Available at: https://www.sciencelearn.org.nz/resources/1675-nanofibres-are-nanoscale-materials (accessed: 23 September 2024).
60. Graham K., Ouyang M., Raether T., Grafe T., Mc Donald B., Knauf P. Polymeric Nanofibers in Air Filtration Applications, 5th Annual Technical Conference & Expo of the American Filtration & Separations Society, Galveston, Texas, April 9–12, 2002.
61. Kattamuri S. B., Potti L., Vinukonda A., Bandi V., Chagantipati S., Mogili R. K. Nanofibers In Pharmaceuticals – A Review. American Journal of PharmTech Research 2012, 2 (6). Available at: http://www.ajptr.com/.
62. Liu Y., et al. Mass Production of Hierarchically Designed Engine-Intake Air Filters by Multinozzle Electroblow Spinning. Nano Letters 2022, 22 (11), pp. 4354–4361. https://doi.org/10.1021/acs.nanolett.2c00704
63. Sanyal A., Sinha-Ray S. Ultrafine PVDF Nanofibers for Filtration of Air-Borne Particulate Matters: A Comprehensive Review. Polymers 2021, 13, 1864. https://doi.org/10.3390/polym13111864

64. Ji X., Huang J., Teng L., Li S., Li X., Cai W., Chen Z., Lai Y. Advances in particulate matter filtration: Materials, performance, and application. Green Energy & Environment 2023, 8, pp. 673–697. https://doi.org/10.1016/j.gee.2022.03.012
65. Borojeni I. A., Gajewski G., Riahi R. A. Application of Electrospun Nonwoven Fibers in Air Filters. Fibers 2022, 10, 15. https://doi.org/10.3390/fib10020015
66. Mann-Hummel – wysokowydajne filtry z nanowłókien. Available at: https://truckfocus.pl/nowosci/7520/mann-filter-wprowadza-wysokowydajne-filtry-z-nanowlokien (accessed: 21 September 2024).
67. Jaroszczyk T., et al. Direct flow air filters – a new approach to high performance Engine filtration. Published in Filtration, the international journal for filtration and separation, 2006, 6 (4), pp. 280–286.
68. Grafe T., Gogins M., Barris M., Schaefer J., Canepa R. Nanofibers in Filtration Applications in Transportation, Filtration 2001 International Conference and Exposition, Chicago, Illinois, December 3–5, 2001.
69. Heikkilä P., Sipilä A., Peltola M., Harlin A. Electrospun PA-66 Coating on Textile Surfaces. Textile Research Journal 2007, 77 (11), pp. 864–870. https://doi.org/10.1177/0040517507078241
70. Li L., Frey M. W., Green T. B. Modification of Air Filter Media with Nylon-6 Nanofibers. Journal of Engineered Fibers and Fabrics 2006, 1 (1), pp. 1–22. https://doi.org/10.1177/155892500600100101
71. Sun Z., Liang Y., He W., Jiang F., Song Q., Tanga M., Wang J. Filtration performance and loading capacity of nano-structured composite filter media for applications with high soot concentrations. Separation and Purification Technology 2019, 221, pp. 175–182. https://doi.org/10.1016/j.seppur.2019.03.087

УДК 621

ПРОБЛЕМИ ФІЛЬТРАЦІЇ ВПУСКНОГО ПОВІТРЯ ДВИГУНІВ ВНУТРІШНЬОГО ЗГОРЯННЯ ТРАНСПОРТНИХ ЗАСОБІВ

Тадеуш Дзюбак[1]; Ян Дізо[2]

[1]Військова політехніка, Варшава, Польща
[2]Жилінський університет, Жилін, Словаччина

Резюме. *Досліджено проблему фільтрації повітря, що надходить у двигуни внутрішнього згоряння транспортних засобів. Основним забруднювачем є мінеральний пил, зокрема діоксид кремнію (SiO_2) та оксид алюмінію (Al_2O_3), які спричиняють інтенсивне абразивне зношування деталей двигуна. Фільтрація повітря здійснюється за допомогою повітряних фільтрів, найпоширенішим типом яких є одноступінчасті фільтри з гофрованим фільтрувальним папером. Однак такі фільтри мають низьку ефективність затримання пилу менше 5 мкм, що є критичним для збереження ресурсу двигуна. Проаналізовано характеристики традиційних матеріалів (целюлозних, поліестерових), а також сучасні композитні рішення з використанням нанофібр. Показано, що застосування нанофібр, виготовлених методом електроспінінгу, значно підвищує ефективність фільтрації дрібнодисперсного пилу. Окрему увагу приділено інноваційним фільтрам PowerCore з аксіальним потоком повітря, що дозволяють зменшити габарити фільтра, знизити втрати тиску та підвищити ресурс. Фільтри з нанофібрами скорочують початковий період низької ефективності, підвищуючи загальний ступінь очищення. Представлено результати експериментів, які демонструють вищу ефективність фільтрів із нанофібрами порівняно з традиційними. Найбільшу шкоду завдають частки пилу діаметром 5–20 мкм, тому фільтрація часток розміром понад 1 мкм є критично важливою. Також розглянуто механізми утримання пилу в пористих середовищах – інерційний, дифузійний, гравітаційний та сита. Комплексна дія цих механізмів забезпечує очищення повітря в двигуні. Показано, що вибір фільтра має враховувати допустиму швидкість фільтрації, геометрію вставки, параметри матеріалу й умови експлуатації. Наголошено на важливості дослідження нових матеріалів для зменшення зношування та продовження терміну служби двигунів.*

Ключові слова: *забруднення повітря, двигуни внутрішнього згоряння, повітряний фільтр, ефективність розділення, поглинання пилу, точність фільтрації, перепад тиску.*

https://doi.org/10.33108/visnyk_tntu2025.02.020 *Received 09.01.2025*